Wavelength selection in one-dimensional cellular structures

Y. Pomeau, Stéphane Zaleski

Tome 42 N° 4 AVRIL 1981

LE JOURNAL DE PHYSIQUE

J. Physique **42** (1981) 515-528 AVRIL **1981**, PAGE 515

Classification
Physics Abstracts
03.40G

Wavelength selection in one-dimensional cellular structures

Y. Pomeau and S. Zaleski (*)

Division de la Physique, Service de Physique Théorique, CEN Saclay, B.P. N° 2, 91190 Gif-sur-Yvette, France

(*Reçu le 4 juillet 1980, accepté le 23 décembre 1980*)

Résumé. — Nous montrons dans des modèles unidimensionnels que la sélection du nombre d'onde dans des structures cellulaires est due aux conditions aux limites qui se font sentir dans toute la structure. Différentes prédictions sont faites en ce qui concerne la dépendance du nombre d'onde dans la longueur de la solution et dans le paramètre de contrôle.

Abstract. — We show on one-dimensional model equations that the wavelength selection in cellular structures is due to the effect of boundary conditions that propagate throughout the whole structure. Various predictions are made concerning the dependence of the wavenumber as a function of the total length of the solution and of the control parameter.

1. **Introduction.** — In his famous article on the convection currents in a horizontal layer of fluid, Lord Rayleigh [1] not only solved the linear problem in a fluid between differentially heated horizontal plates, he also settled the problem of the pattern selection as follows : « the cells of Bénard [2] are then reduced to infinitely long strips, and, when there is instability, we may ask for what wavelength the instability is greatest. The answer can be given under certain restrictions, and the manner in which equilibrium breaks down is then approximately determined. So long as the 2-dimensional character is retained, there seems to be no reason to expect the wavelength to alter afterwards ». If one interprets this suggestion of Lord Rayleigh as meaning that the wavenumber selected is the one with the maximal linear growth rate, it is in contradiction with the most careful observations, made in particular by Koschmieder [3] : beyond the onset of convection, there is a natural tendency for the wavelength to increase, at least for large Prandtl number fluids where most experiments, by visual observation of the convective pattern are done.

This wavelength increase is, of course, not seen in experiments where the wavelength is imposed from the outside, for instance by a periodic horizontal differential heating [18]. This last circumstance is likely a source of misunderstanding : a confusion seems to exist between the problem of stability of patterns with an imposed wavelength, and the problem of the « natural » evolution of a pattern without, *a priori*, any imposed structure, except (possibly) the one due to the vertical boundary conditions.

Up to now, the origin of this wavelength increase remains unclear. However it is of interest to understand it as experiments on convection in various fluids reveal [4] that, near the onset of convection, a low frequency turbulence develops in large structures, indicating that the selected convective pattern might be spontaneously unstable with respect to slow displacements of the structure [5]. A source of difficulty here could be the well known fact [6] that the Rayleigh-Bénard convection at threshold takes place after a normal (or « supercritical ») bifurcation, and this implies in a *certain sense* that the convective flow must be stable in slightly supercritical conditions. A careful

(*) Laboratoire de Physique du Solide, ENS, 24, rue Lhomond, Paris, France.

examination of the arguments leading to this conclusion show that its truth requires either the assumption that the pattern is infinite and periodic with a *definite* and *imposed* period, or that convection takes place in a finite box. Of course, experimental convection takes place in finite (even large) boxes, but the region of stability that is determined by the general theorems of stability of supercritical bifurcations shrinks to zero (in the range of supercritical Rayleigh number) as the size of the system goes to infinity. Essentially, this sort of theory is limited by the phase motions, yielding very small rates of change of order L^{-2} when the size of the pattern L goes to infinity. The question of these phase motions in cellular flows has been considered elsewhere [7] and it has been shown that they are described by diffusion equations, some diffusion constant being negative if the underlying structure is unstable against this sort of motions. Daniels and Hall and Walton have considered [21] the effect of a small heat transfer through lateral boundaries. This makes the sharp transition from conduction to convection disappear. In that follows we shall not consider this sort of effect, and limit ourselves to models with a sharp transition.

The present paper reports on studies of model equations in one-dimension. This was made with the intent of showing that wavelength selection is likely due to boundary effects ([1]). This has been felt by a number of investigators in the field, although it does not seem to have been already stated explicitly in the literature. That the wavelength selection originates from boundary effects is, after all, not surprising. If one thinks of macroscopic crystals in their ground state under a positive pressure, the interparticle spacing is a well defined function of this external pressure. However, as we shall see in our model equation, a quite subtle competition may take place between the tendency to accomodate the boundary conditions and the tendency to fall into the ground state (when this notion has a meaning), which implies a well defined interparticle spacing.

We do not claim to have solved the general problem of wavenumber selection in cellular flows, but at least we give a rather precise explanation of what happens in one model. In the conclusion, we shall discuss possible implications of our results, regarding in particular the obvious limitations of models with respect to the real (and thus much more complicated) situations.

The rest of this paper is organized in four parts, of which we shall now give some details. We shall simultaneously present some of the ideas to be developed.

In part 2, we introduce two model equations (models « a » and « b ») and outline some of their elementary properties. The models considered are two non linear partial differential equations for a function $A(x, t)$. They are of first order with respect to t (« time ») and of fourth order with respect to x (« space »). These equations depend on a control parameter denoted as ε. The control parameter ε is defined in such a way that if it is less than zero, the only stable solution is $A = 0$, although for ε a slightly larger than zero, steady (= time independent) solutions periodic with respect to x exist. These steady solutions are studied in the rest of the paper by perturbation theory near $\varepsilon = 0$.

In part 3, we consider how steady periodic solutions « accomodate » the boundaries, the boundary conditions being chosen to be $A = \partial A/\partial x = 0$. The periodic solutions do not fit the boundary conditions, and a boundary layer joins the boundary to the periodic pattern if its size is much larger than the space period. We first discuss the existence of this boundary layer from a geometrical point of view. Considering only steady-state solutions (as done in the rest of the paper), we find for models a and b two systems of fourth order ordinary differential equations (with respect to x), which can be also considered as four non linear differential equations of first order. We discuss the « phase portrait » of the corresponding flow in $\mathbb{R}^4$.

Steady semi-infinite solutions exist which satisfy the boundary conditions at $x = 0$ ($A = \partial A/\partial x = 0$) and are periodic as $x \to +\infty$. These solutions are given by the intersection of two surfaces in $\mathbb{R}^4$: one of these surfaces is defined by the boundary conditions, the other one is the stable manifold of one of the closed trajectories describing periodic solutions : any point starting in this manifold tends asymptotically to the periodic solution. This geometrical approach has been followed to obtain numerical results giving what is drawn in figures 1 to 3a : considering the four first order differential equations (with respect to x), we have sought the initial conditions yielding steady solutions either in a finite (and large) box or in a semi-infinite layer.

Subsection (3.1.a) is self contained, and is devoted to the computation (near $\varepsilon = 0_+$) of the band of wavenumber selected in semi-infinite solutions for model a. This perturbative calculation uses two ingredients : the steady solutions are the Euler-Lagrange of a functional $V[A]$. Accordingly an invariant quantity exists, formally analogous to an energy, V being the Lagrange function. This invariant, denoted as K, depends on the local values of A and its first, second and third derivatives, and it satisfies $dK/dx = 0$. Indeed this relates the solution $A(x)$ at the boundary and in the bulk, as K must be constant everywhere. The perturbative computation of K for periodic solutions far from the boundary is trivial near $\varepsilon = 0_+$. The computation of K at the boundary is done by means of envelope theory [14]. Near the boundary, the amplitude of the solution is small and the linear approximation is valid, so that the solution is readily obtained except for a general multiplicative

([1]) This effect was recently discussed by Cross *et al.* [8], for both the Boussinesq equations and the models of reference [5] considered here.

factor. This factor is found (near $\varepsilon = 0_+$) by a matching condition. The slope of the envelope at the boundary is determined in two different ways : first it is the derivative of the hyperbolic tangent of the envelope theory, and it is also given in the linear approximation, since this gives the solution as a linear superposition of two oscillations with opposed amplitudes and very close wavenumbers. Once the amplitude of the linear solution at the boundary is fixed, the boundary conditions leave an undetermined phase called φ. When this phase changes a corresponding variation is induced into the invariant K. As K at infinity (and for ε fixed) depends on the wavenumber only, the variation of φ is transformed into a variation of the wavenumber at infinity. This is the way in which the wavelength is selected in a narrow band for model *a*.

Wavenumber selection in model *b* is examined in subsection (3.1.*b*). The computation is very similar to the one of subsec. (3.1.*a*), except that it requires an « adiabatic » invariant instead of the exact invariant K of a model *a*. The derivation of this invariant is given in appendix B.

In subsec. (3.2), we use the results of subsec. (3.1) to determine the pattern selection in *finite boxes* of length L (instead of semi-infinite geometries considered previously). The method used for this is the study of solutions at fixed ε when L increases. It is based upon an examination of figures 3*a* and 3*b*. One of the results is that at small ε and large εL, the number of steady solutions is of order (εL).

In section 4 we present some remarks concerning various points raised by our results. For more realistic problems, such as the wavelength selection for Rayleigh-Bénard convection in large boxes, we show that there is some indication that the boundary layer is unstable against a localized cross-roll instability when the rolls are parallel to this boundary. This probably makes quite difficult a theoretical approach to wavenumber selection in this case, if one follows the method of the present paper. However, in elasticity problems [19] or for free thermoconvection in porous layers [20], it is possible, at least in principle, to test the ideas presented in the present paper.

2. **Models and their elementary properties.** — For a reason which will appear later we have restricted our attention to two models of cellular flow. As emphasized elsewhere [7], these models imply obvious idealizations with respect to realistic equations for cellular flows. We shall refrain for the moment of discussing the consequences of this idealization and give the model equations.

Let $A(x, t)$ be a (smooth) function of x (space) and t (time). We consider the non linear partial differential equations

$$A_t = \Omega_\varepsilon A - A^3 \tag{1a}$$

$$A_t = \Omega_\varepsilon A - AA_x \tag{1b}$$

where $A_u \equiv \partial A/\partial u$ $(u = x, t)$, $\Omega_\varepsilon \equiv \varepsilon - (\partial_{x^2}^2 + q_0^2)^2$, q_0 being an (arbitrary) wavenumber. These equations have to be supplemented by boundary conditions [except, of course, for the case of periodic solutions such that $A(x + L) = A(x)\ \forall x$], but we shall not consider this last case, which is markedly different of the one which we shall consider. We have chosen to study these equations for $0 < x < L$ with the b.c.

$$A = A_x = 0 \quad \text{for} \quad x = 0 \quad \text{and} \quad L .$$

Consider now, as usual, steady solutions of (1) in the form sin (qx). One readily finds that fluctuations of this form are linearly unstable around the steady solution $A = 0$ in the range

$$q \in [(q_0^2 - \varepsilon^{1/2})^{1/2},\ (q_0^2 + \varepsilon^{1/2})^{1/2}] \text{ if } \varepsilon > 0 .$$

Of course, these solutions do not fit the b.c. whatever L is, and we shall be concerned now with the influence of b.c.

In the limit of an infinite one-dimensional pattern, the bifurcation from the solution $A = 0$ to a non zero solution as ε becomes positive is supercritical, since a steady non zero solution may be found by perturbation in the range $\varepsilon > 0$ only. The perturbative construction of these steady solutions is quite elementary and need not to be explained here.

One finds from (1*a*)

$$A^{(0)}(x) = a_0 \sin qx + a_1 \sin 3\,qx + \cdots \tag{2a}$$

where

$$a_0 \simeq \pm \left(\frac{4\,\gamma(q)}{3}\right)^{1/2}, \qquad a_1 \simeq -\frac{a_0^3}{4\,\gamma(3\,q)}$$

and from (1*b*)

$$A^{(0)}(x) = a'_0 \sin qx + a'_1 \sin 2\,qx + \cdots \tag{2b}$$

where

$$a'_0 = \pm \left(\frac{-4\,\gamma(q)\,\gamma(2\,q)}{q^2}\right)^{1/2} \quad \text{and} \quad a'_1 = \frac{-2\,\gamma(q)}{q} .$$

In all these expansions $\gamma(z)$ is the linear damping (or growth) rate of fluctuations with wavenumber z : $\gamma(z) \equiv \varepsilon - (z^2 - q_0^2)^2$, and the perturbation solution requires $0 < \gamma(q) \ll 1$.

It is of interest to notice that, despite the fact that the non linear term is formally quadratic w.r.t. A in (1*b*), no subcritical solution exists [6]. This is connected with the peculiar form of this quadratic term, allowing an « energy principle » : multiplying both sides of (1*b*) by A and integrating either over a space period (in the case of periodic solution in an infinite layer) or over the « length of the box » (in the case of a solution between 0 and L), one eliminates by partial integration the contribution of the non linear terms to the time derivative of the energy :

$$\frac{\mathrm{d}}{\mathrm{d}t}\int A^2\,\mathrm{d}x = \int A(\Omega_\varepsilon A)\,\mathrm{d}x \tag{3}$$

if ε is negative, the operator Ω_ε is negative, and $\int A^2\,dx$ can only decrease.

To prove in general that (1*a*) has a supercritical bifurcation from the rest state $A = 0$, is almost as easy, since one adds $-\int A^4\,dx$ to the r.h.s. of (3), which is negative.

Owing to its peculiar form (1*a*) has strong stability properties. These stability properties are typical of a quite general class of such non linear equations, where A^3 is replaced by $-\frac{dU(A)}{dA}$, $U(.)$ being an even smooth function with an absolute minimum at zero. Instead of considering this general class of systems, at the price of awkward algebraic manipulation, we have chosen to look at this peculiar case; the extension to a more general U is obvious. Let us define the functional

$$V[A] = \int dx\left[\frac{A^4}{4} - \frac{\varepsilon A^2}{2} + \frac{A_{xx}^2}{2} - q_0^2 A_x^2 + \frac{q_0^4}{2} A^2\right]. \tag{4}$$

Thus (1*a*) can be put into the form

$$A_t = -\frac{\delta V}{\delta A}, \tag{5}$$

where $\delta/\delta A$ is the Fréchet derivative. The above form of the equation of the motion shows that $V[A]$ decreases monotonously as time goes on (this reasoning is valid either for solutions on a bounded interval or for solutions with a prescribed space period). To show that $V[A]$ is bounded from below, let us define the L^4 norm of A as

$$\| A \| \equiv \left[\frac{1}{L}\int_0^L dx A^4\right]^{1/4}.$$

From the Cauchy-Schwarz inequality

$$\frac{1}{L}\int_0^L A^2\,dx \leqslant \| A \|^2$$

and

$$\frac{1}{L}\int_0^L dx\left(\frac{A^4}{4} - \frac{\varepsilon A^2}{2}\right) \geqslant \frac{1}{4}\| A \|^4 - \frac{\varepsilon}{2}\| A \|^2;$$

furthermore since

$$\int_0^L \frac{dx}{2}(A_{xx}^2 - 2 q_0^2 A_x^2 + q_0^4 A^2) = \int_0^L dx A[(\partial_{x^2}^2 + q_0^2)^2 A],$$

one has

$$L^{-1} V[A] \geqslant \frac{1}{4}\| A \|^4 - \frac{\varepsilon \| A \|^2}{2}$$

and

$$L^{-1} V[A] \geqslant -\varepsilon^2/2.$$

One of the purposes of this paper is to establish the nature of the ground state; that is, the shape of A making V minimum, given L and ε. This ground state is of course a stable steady state, and the existence of a variational formulation for (1*a*) excludes the possibility of sustained oscillations.

From this point of view, the case of (1*b*) is much more generic as no Lyapunov functional exists for $\varepsilon > 0$. In particular, numerical experiments [9] on (1*b*) indicate that sustained oscillations appear spontaneously in large structures beyond some well definite threshold. This shows that no « hidden » variational formulation exists for (1*b*). One may think that this is also the case for the non linear time dependent equations of hydrodynamics. This point is of interest, since the idea that some sort of « preferred » wavenumber exists for cellular flows in supercritical conditions should result from a variational formulation of these hydrodynamical equations. For instance, it has often been suggested that the convection flow in R.B. experiments tends to maximize the heat flow.

3. **Outline of the calculations. Results.** — Having in mind the results of dynamical simulations of (1*a* and *b*) we have asked if the final steady state obtained near $\varepsilon = 0_+$ was a consequence of some dynamical selection process, connected for instance with the stability of the structure of the steady solutions of (1*a* and *b*) in a large box. That is why we have tried to find the whole set of steady solutions in a large box, without worrying about their *dynamical stability*. On the basis of numerical calculations, it was shown in reference [5] that a selected steady one-dimensional pattern may be linearly *unstable* against some sort of perturbations. This gives a concrete support to the idea [5] that the low frequency turbulence observed [4] near threshold in Rayleigh-Bénard convection is due to the selection of a structure with an unstable wavenumber.

The steady solutions are the solutions of the fourth order ordinary differential equations

$$A_{x^4} + 2 q_0^2 A_{xx} + q_0^4 A = \varepsilon A - (A^3 \quad \text{or} \quad A A_x) \tag{6}$$

with the b.c. $A = A_x = 0$ at $x = 0$ and L.

A simple calculation shows that a non trivial solution of (6) exists if L is larger than a quantity of order $\varepsilon^{-1/2}$ near $\varepsilon = 0$.

We have considered (6) as defining a flow in $\mathbb{R}^4$: consider x as a time and define the vector (A_1, A_2, A_3, A_4) that depends on this « time » as

$$\begin{aligned} A_{1,x} &= A_2 \\ A_{2,x} &= A_3 \\ A_{3,x} &= A_4 \\ A_{4,x} &= \varepsilon A_1 - (A_1^3 \quad \text{or} \quad A_1 A_2) - q_0^4 A_1 - 2 q_0^2 A_3 . \end{aligned} \tag{7}$$

Due to the boundary conditions, we are looking for solutions of this system starting at « time » zero from the 2-plane $A_1 = A_2 = 0$ (which will be called P_2 from now on), and returning after a « time » L.

Among these solutions, a particularly important class is made of what can be called the « regular » ones. They are as follows : boundary layers (of width $\varepsilon^{-1/2}$ near $\varepsilon = 0$) exist near $x = 0$ and near $x = L$, and in between the regular solution possesses very regular oscillations. At large L, the wavelength of this solution can be appreciated with a relative accuracy much better than L^{-1}, contrary to what could be expected from simple arguments. This is because the convergence to the regular oscillations from the boundary layer to the bulk is exponential, so that perturbations in the bulk due to finite size effects are of order $\exp -(k\varepsilon^{1/2} L)$, where k is some constant. In computer experiments, the indeterminacy in the wavelength due to finite size effects becomes, as L grows beyond, say ten times q_0^{-1}, of the same order or smaller than the round off errors and/or the finite mesh effects.

Before examining in the following subsection 3.2 the construction of solutions for a large finite L, we shall look in subsection 3.1 at the problem of solutions in a half-infinite line; that is, solutions starting from the 2-plane $A_1 = A_2 = 0$ and tending asymptotically to a periodic solution after some transients. Solutions with large, but finite L, are made in some sense by gluing together two half-infinite solutions.

3.1 HALF-INFINITE SOLUTIONS. — In what follows, we call simple closed trajectory (in short SCT) the closed trajectories in $\mathbb{R}^4$ with a wavenumber in the unstable band $](q_0^2 - \varepsilon^{1/2})^{1/2}, (q_0^2 + \varepsilon^{1/2})^{1/2}[$; they are « simple » in the sense that they can be obtained near $\varepsilon = 0_+$ by perturbation, as shown in equations (2*a* and *b*). More complex closed trajectories exist. Near threshold ($\varepsilon = 0_+$) they can be described as periodic solutions of period of order q_0^{-1}, which are slowly modulated with a much longer period. These modulated solutions can be understood basically in the same way as the half-infinite solution, the modulation effect being due to the occurrence of internal boundaries, as it will be discussed thereafter.

To understand the way in which this SCT can be reached from the outside (in particular from the « initial » or « boundary » conditions $A = A_x = 0$, that is from P_2), one must first study the local structure of the flow around this SCT : do real trajectories exist which are asymptotic to SCT ? Then one must wonder if a subset of these asymptotic trajectories cut the manifold of initial conditions, making possible a half-infinite solution. A picture of this situation is given in figures 1*a* and 1*b*, where we draw the Poincaré map obtained from the cuts of trajectories with the 3-space H_3^+ defined in $\mathbb{R}^4$ by $A_x = 0$ and $q_0^2 A - A_{xx} < 0$.

The first question can be answered by determining the local structure of the flow defined by (7) around the SCT. This can be done, as explained in Appendix A by a Floquet-expansion.

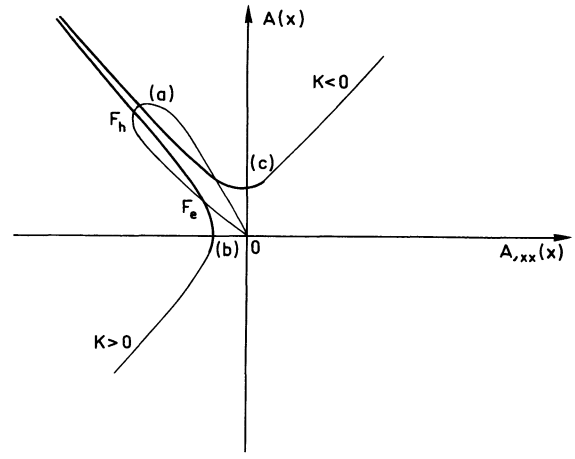

Fig. 1*a*. — This is the Poincaré map in the half space H_3^+. Line (*a*) is made of the intersections of the SCT (simple closed trajectories) with H_3^+. Line (*b*) is an example of the trace of a stable manifold starting from a hyperbolic fixed point F_h and cutting the $A = 0$ plane, although line (*c*) is the trace in H_3^+ of a stable manifold which does not cut the $A = 0$ plane and thus does not belong to a SCT attainable from P_2.

The main result of this calculation is that near $\varepsilon = 0_+$, the SCT are *hyperbolic* in the region of wavenumber stable with respect to the Eckhaus instability [10] (no confusion must be made with the

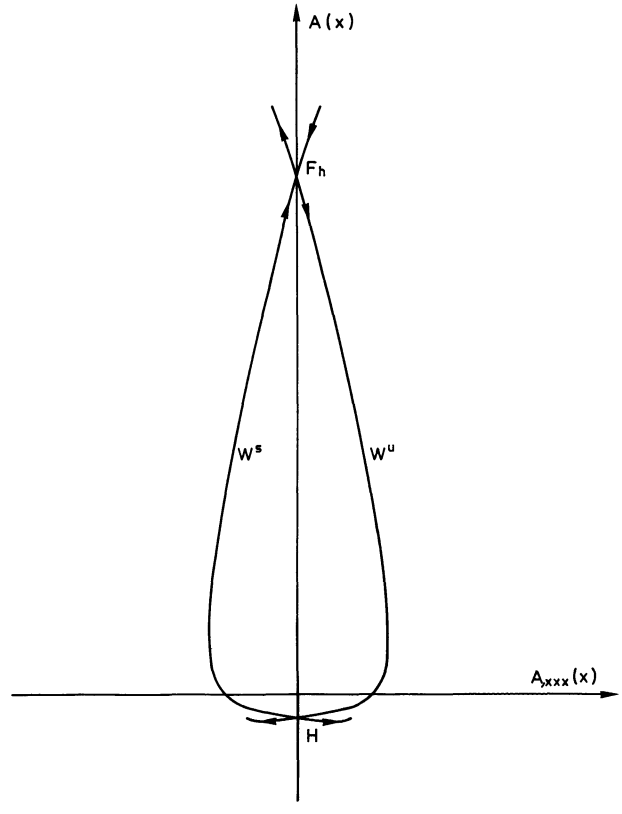

Fig. 1*b*. — Projection (parallel to the coordinate A_{xx}) of the stable (W_s) and unstable (W_u) manifolds of a hyperbolic trajectory. W_s and W_u intersects at H which is a homoclinic point.

Eckhaus instability, which refers to stability in the usual sense — that is, for the time dependent equations — although we shall consider hereafter the *stable* and *unstable* manifolds of SCT, for which the word « stability » refers to these equations of motion in x-space). For these hyperbolic SCT two surfaces (or « manifolds » in the usual mathematical terminology) exist, often called W_s and W_u (s and u for stable and unstable respectively) with the following properties.

i) Both W_u and W_s are globally invariant under the equation of motion (in the x-space of course) : a point starting in W_u (or W_s) and obeying the equations of motion (7) remains forever in W_u (W_s). As explained in Appendix A, W_u and W_s are 2-dimensional.

ii) The SCT is at one of the intersections of W_u and W_s. There is a one-dimensional continuum of such manifolds, as a 1-d continuum of SCT exists for $\varepsilon > 0$; this continuum is indexed, for instance, by the space period of any Eckhaus stable periodic solution.

iii) Any trajectory starting in W_s (resp. W_u) is asymptotic at $x \to + \infty$ (resp. $x \to - \infty$) to the corresponding SCT.

As explained in Appendix A, this hyperbolic character of the Eckhaus stable SCT is a simple consequence of the real character of the corresponding Floquet exponents.

As shown in Appendix A, the Eckhaus unstable SCT are on the contrary elliptic : that is no neighbouring trajectory tends to them. These elliptic trajectories are surrounded by a continuum of nested tori, on which neighbouring trajectories wind up undefinitely, as familiar now from the KAM theorem [11]. These elliptic SCT cannot be reached from initial (or boundary) conditions which are not precisely on them. In Aubry's terminology [12], these elliptic trajectories are not defectible, although the hyperbolic ones are defectible, the defect being here simply the transient going from rather arbitrary initial conditions to a SCT.

However, as said above, the « local » structure of the flow around a SCT is not sufficient to determine if this SCT can be reached from P_2. To be accessible from a starting point in P_2, a SCT must have its stable manifold W_s cutting it. As we shall see, this is a very restrictive condition, and defines a narrow band, of width of order ε (near $\varepsilon = 0_+$) in the band of hyperbolic SCT, which is itself of width of order $\varepsilon^{1/2}$.

To detail and justify these last statements, it is better to consider separately the case of (1*a*) and (1*b*).

3.1.*a*. — Let us recall that we are solving the fourth order ordinary differential equation

$$\varepsilon A - (\partial_{x^2}^2 + q_0^2)^2 A = A^3 .$$

Multiplying by A_x, one finds the constant of the motion

$$K[A] = \frac{\varepsilon A^2}{2} - \frac{q_0^4}{2} A^2 - q_0^2 A_x^2 - A_x A_{xxx} + \frac{1}{2} A_{xx}^2 - \frac{A^4}{4} . \tag{8}$$

In the plane of the boundary conditions ($A = A_x = 0$) the value of the constant of the motion is $\frac{1}{2} A_{xx}^2$, so that, to be accessible from a starting point with

$$A = A_x = 0 ,$$

a SCT must have a positive constant K. This gives a first condition of wavenumber selection.

In the present case, this condition seems to be bound to the existence and form of the constant of the motion. But this is only partly true. Actually, the limit SCT defined in this way is reached from initial conditions $A = A_x = A_{xx} = 0$.

Let us consider the corresponding half-infinite solution, say $A^{(0)}$ and let Λ be the linear operator obtained by linearizing the equations of motion around $A^{(0)}$: acting on an arbitrary function $\tilde{A}(x)$, Λ is defined as

$$\Lambda \tilde{A}(x) \equiv \Omega_\varepsilon \tilde{A}(x) - 3(A^{(0)})^2 \tilde{A}(x) .$$

As the equation of motion is autonomous with respect to x (i.e. formally invariant in the change

$$x \to x + x_0 ,$$

x_0 arbitrary length) $A_x^{(0)}$ is formally an eigenfunction of Λ with eigenvalue 0. But in general, $A_x^{(0)}$ does not satisfy the prescribed b.c. This happens only when

$$A_x^{(0)} = (A_x^{(0)})_x = 0 ,$$

that is if $A_{xx}^{(0)} = 0$ and corresponds precisely to the limit SCT, as defined above.

As it is well known from bifurcation theory [13], the occurrence of a non trivial kernel in a linearized functional problem denotes a bifurcation. To make this more concrete, one may reason as follows : Each SCT has a two-dimensional stable manifold W_s and, as the 2-plane P_2 is also 2-dimensional, the intersection of a W_s and P_2 is made of a finite number of points, so that the 1-d continuum of W_s manifolds cuts P_2 along a curve, say Γ (or eventually along a discrete set of curves) which may be drawn in the cartesian plane (A_{xx}, A_{xxx}) (see Fig. 3*a*).

The existence of the above bifurcation at $A_{xx}^{(0)} = 0$ implies that Γ is perpendicular to the axis $A_{xx} = 0$ at their mutual intersection. This bifurcation also occurs in any « generic » parametrization of the half-infinite solutions (that is, near the bifurcation point, the parameter must define a transverse intersection at the critical point).

This bifurcation can be seen for instance in the parametrization defined by the final wavenumber of the SCT to which tends a half-infinite solution. Thus it is natural to expect that one of the limit of « attainable » SCT in the wavenumber space corres-

ponds precisely to a starting point in P_2 with $A_{xx}=0$. To understand the other limit for the selected wavenumber, one may use the following remarks.

One of the possible ways to attack the problem is envelope theory [14, 8] ; near $\varepsilon = 0_+$ the solution of the original equations is a product of a rapidly varying function and of a smooth function. In the present case, the rapidly varying function is periodic with space period q_0, and the sought form for A has the form

$$A = \chi(x) \sin (q_0 x + \psi) .$$

$\chi(x)$ being slowly varying (on the space scale $2\pi/q_0$) and ψ an arbitrary phase. A straighforward calculation shows that $\chi(x)$ obeys the equation

$$\varepsilon\chi - \frac{3}{4}\chi^3 + 4 q_0^2 \chi_{xx} = 0 . \qquad (9)$$

The solution of this equation describing the boundary layer for the half-infinite problem is

$$\chi(x) = \pm \left(\frac{4\varepsilon}{3}\right)^{1/2} \tanh\left[x\left(\frac{\varepsilon}{8 q_0^2}\right)^{1/2}\right]; \qquad (10)$$

it satisfies the boundary conditions (i.e. $A = A_x = 0$ at $x = 0$) if $\psi = 0$, the next derivatives being

$$A_{xx}|_{x=0} = (\tfrac{2}{3})^{1/2} \varepsilon \quad \text{and} \quad A_{xxx}|_{x=0} = 0 .$$

In the geometrical formulation, envelope theory allows one to know the stable (and unstable) manifolds of our particular SCT (the one with period q_0).

A consequence of this calculation is the fact that near $\varepsilon = 0_+$ the invariant K is of order ε^2, so that near P_2, the non linear term is negligible. This allows one to determine the above defined curve Γ (= the trace of the stable manifolds of the accessible SCT in P_2).

Actually, in the linear approximation, and for ε given, the general solution of (6) is a superposition of two circular function with wavenumber $q_\pm = (q_0^2 \pm \varepsilon^{1/2})^{1/2}$:

$$A(x) = \sum_{i=\pm} a_i \sin (q_i x + \varphi_i) \qquad (11)$$

where a_i, φ_i are four arbitrary numbers. The boundary conditions put the following conditions on them :

$$(A|_{x=0} \equiv) \sum_{i=\pm} a_i \sin \varphi_i = 0$$

and

$$(A_x|_{x=0} \equiv) \sum_{i=\pm} a_i q_i \cos \varphi_i = 0 .$$

This gives for $\varphi_\pm$:

$$\frac{1}{q_-} \tan \varphi_- = \frac{1}{q_+} \tan \varphi_+ .$$

From $q_- \approx q_+$ one gets the estimates :

$$\varphi_- - \varphi_+ \simeq \frac{2\varepsilon^{1/2} q_0^{-2}}{\sin 2\varphi_+} \quad \text{and} \quad a_+ \approx -a_- ,$$

so that

$$A_{xx}|_{x=0} \simeq -2 a_+ \varepsilon^{1/2} \sin \varphi_+$$

$$A_{xxx}|_{x=0} \simeq -2 a_+ q_0 \varepsilon^{1/2} \cos \varphi_+$$

and

$$q_0^2 (A_{xx}|_{x=0})^2 + (A_{xxx}|_{x=0})^2 \simeq 4 a_+^2 \varepsilon q_0^2 . \qquad (12)$$

But a_+ is constant on Γ (so that Γ is a circle in P_2). This can be shown as follows : the solution given by (11) is made of fast oscillations of period q_0 times a slowly varying envelope $2 a_+ \sin(\frac{1}{2}(q_+ - q_-) x)$. This envelope must match the « outer » envelope obtained from the non linear theory. The derivative of the outer envelope at $x = 0$ is

$$\left(\frac{4\varepsilon}{3}\right)^{1/2} \left(\frac{\varepsilon}{8 q_0^2}\right)^{1/2} = 6^{-1/2} \varepsilon/q_0 ,$$

so that the matching of this first derivative with the above linear solution at $x = 0$ yields

$$a_+(q_+ - q_-) \simeq 6^{-1/2} \varepsilon/q_0 .$$

As the non linear envelope equation differs appreciably from (10) (that is obtained when the underlying wavenumber is q_0) only for wavenumber differing from q_0 of an order $\varepsilon^{1/2}$, and as we are interested in wavenumber such that $q - q_0 \sim 0(\varepsilon)$, the above matching condition shows that near $\varepsilon = 0_+$, the quantity a_+ does not depend on the wavenumber of the SCT merging from an arbitrary point on Γ, so that from (12), Γ is a circle.

To delineate now the range of wavenumbers of the SCT merging from Γ, the simplest thing to do is to use the invariant K and to connect it to the above deduced value of a_+.

A straightforward calculation gives the following expression for the invariant computed for the SCT as a function of the wavenumber :

$$K \simeq \frac{\varepsilon}{3}\left(\frac{\varepsilon}{2} + 8 q_0^3 \delta\right)$$

where $\delta \equiv q - q_0$, and where we have neglected terms of order ε^3, $\varepsilon\delta^2$, ...

The limit value $K = 0$ is reached for $\delta_- = \dfrac{-\varepsilon}{16 q_0^3}$; it corresponds in the band of accessible wavenumber to the one with the boundary condition $A_{xx} = 0$.

The other limit is reached for $A_{xxx} = 0$, and corresponds to $K = 2 a_+^2 \varepsilon$, since it is realized for

$$A_{xx}|_{x=0} = 2 a_+ \varepsilon^{1/2} , \quad A_{xxx}|_{x=0} = 0 ,$$

and since $K = \frac{1}{2} A_{xx}^2$ on P_2. A simple substitution

of the above defined a_+ gives $\delta_+ = \frac{\varepsilon}{16\, q_0^3}$ for this limit of the accessible wavenumber.

The main conclusion of these considerations is that, near $\varepsilon = 0_+$, the half-infinite solutions have a wavenumber in the band

$$[q_0 + \delta_-(\varepsilon),\, q_0 + \delta_+(\varepsilon)]\,,$$

where $\delta_\pm(\varepsilon) \underset{\varepsilon \to 0_+}{\simeq} \pm \frac{\varepsilon}{16\, q_0^3}$ [15]. The symmetry of this band is seemingly an accident. Moreover, all the above considerations are in perfect agreement with our numerical calculations (Fig. 2*a*).

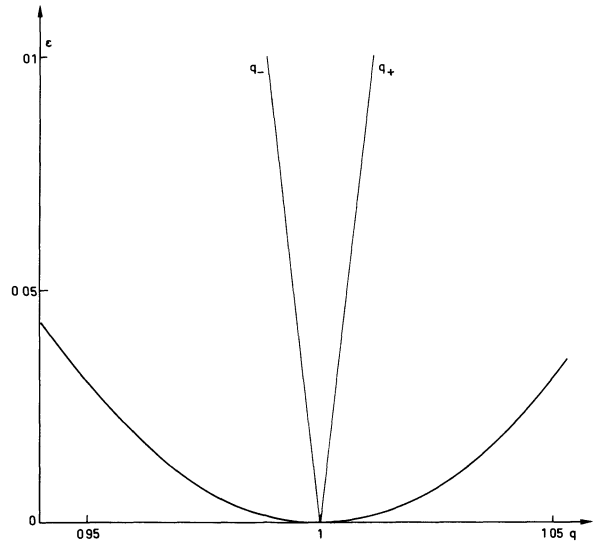

Fig. 2*a*. — The band of wavenumbers $]q_-(\varepsilon),\, q_+(\varepsilon)[$ for model (*a*) in the cartesian plane $(q,\, \varepsilon)$.

3.1.*b*. — Many results established for model (*a*) remain *a priori* true for model (*b*) :

$$\varepsilon A - (\partial_{x^2}^2 + q_0^2)^2\, A = A A_x\,. \qquad (13)$$

However, this is not true of the results which require the formal existence of the invariant K.

However, for model (*b*), one may construct near $\varepsilon = 0_+$ an adiabatic invariant playing the role of the exact invariant of (*a*). Its derivation is given in appendix B.

The final result is the value of the invariant [say $J(A)$] : it is $\frac{1}{2} A_{xx}^2$ in P_2 (and near $A_{xx} = A_{xxx} = 0$) and $\frac{159}{2} \varepsilon q_0^2 \left(\varepsilon + \frac{48}{53} q_0^3\, \delta\right)$ for periodic solutions with a wavenumber $q = q_0 + \delta$ and $\delta \sim \varepsilon$. As for model (*a*), $J = 0$ defines one of the boundaries of the range of accessible wavenumbers, this corresponds to

$$\delta_- \simeq -\frac{53}{48} \varepsilon q_0^{-3}\,.$$

The other limit could be computed as for model (*a*) by matching the inner and outer envelope. However another more direct method can be used ; it consists in matching the solution itself.

The envelope equation gives for the dominant part of the solution $A(x) = \chi(x) \sin q_0\, x$, where χ is the solution of

$$\varepsilon \chi + 4\, q_0^2\, \chi_{xx} = \frac{1}{36\, q_0^2}\, \chi^3\,. \qquad (14)$$

The half-infinite solution of (14) is :

$$\chi = \pm\, (36\, \varepsilon q_0^2)^{1/2} \tanh\left(\left(\frac{\varepsilon}{8}\right)^{1/2} \frac{x}{q_0}\right).$$

At $x = 0, A = A_x = A_{xxx} = 0$ and $A_{xx} = 3\sqrt{2}\, \varepsilon q_0$. Thus the maximum value for the invariant P_2 is

$$\tfrac{1}{2} A_{xx}^2 = 9\, \varepsilon^2\, q_0^2\,.$$

Once made equal to the expression for J as a function of $\delta (= q - q_0)$, this gives the other limit value for δ [15], which is

$$\delta_- \simeq -\frac{47}{48} \varepsilon q_0^{-3}\,.$$

Before to close this subsection, let us make two comments :

i) Our numerical computation are in good agreement with the calculated limits for the selected wavenumber (Fig. 2*b*).

ii) The recourse to the adiabatic invariant for computing the solutions may be justified by the following remark (based again upon our numerical calculations). When we are looking at finite (but large) values of L (which is the length of our « box »), the solution must fall at $x = 0$ *and* $x = L$ in P_2 (in more explicit terms, it checks the boundary conditions at the two ends of the box) and we have verified that — near $\varepsilon = 0_+$ — at both ends, the value of A_{xx} are either the same or opposite, which implies that the adiabatic invariant is conserved throughout the whole trajectory.

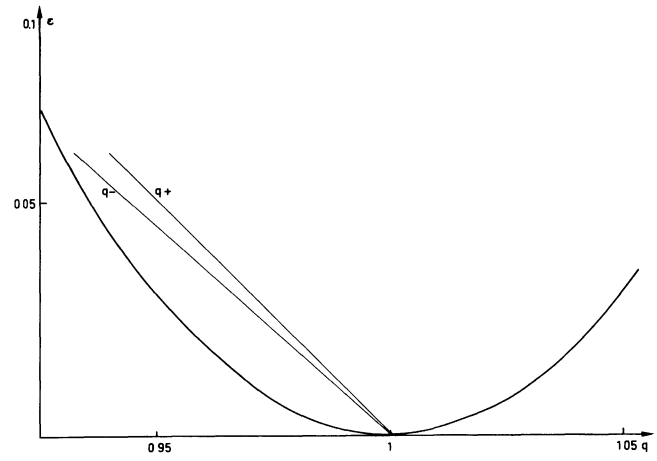

Fig. 2*b*. — Same as figure 2*a* for model (*b*).

3.2 SOLUTIONS IN FINITE BOXES [FOR MODELS (*a*) AND (*b*)]. — As alluded above, these solutions are obtained by « gluing » together half-infinite solutions. In geometrical terms [i.e. by considering trajectories in $\mathbb{R}^4$, as defined by eq. (7)], the starting point is not exactly on Γ ($\equiv$ the intersection of P_2 with the stable manifold W_s of the SCT). Hence, after some « time » the representation point on this trajectory feels the instability of the SCT (this SCT defines the bulk wavelength of the solution) and escapes along the unstable manifold of this SCT. Of course, as the length increases, this escape must occur later and later so that the starting point must be closer and closer to Γ.

The condition for a return to P_2 defines a discrete set of starting points in P_2 for a given SCT (provided, of course, that its stable manifold cuts P_2) : for an arbitrary starting point close to Γ, the set of escaping points (i.e. the ones on W_u) is an arbitrary set of iterates close to W_u as seen from the point of view of the Poincaré map in H_3^+. And, in general, none of these iterates (which are on a line in H_3^+) lies in P_2.

The discrete set of points starting from and returning to P_2 after a stagnation in the vicinity of SCT, accumulate on Γ in a geometric fashion. If one draws by continuity (with respect to the wavenumber of the SCT in the bulk) the set of starting points yielding finite solutions, one gets in P_2 two spirals starting from the point $A_{xx} = A_3 = 0$, each spiral corresponding to a solution of a given parity with respect to the middle of the cell [see Fig. (3*a*)]. These spirals converge exponentially toward the circle Γ, so that the infinite number of neighbouring intercepts of one of them with a line $A_{xx} = C$ correspond to the solution with a bulk wavenumber defined by the value of the invariant. As one gets closer to the limit Γ it is almost obvious that these successive intercepts correspond to a step increase of one wavelength for the total length of the solution.

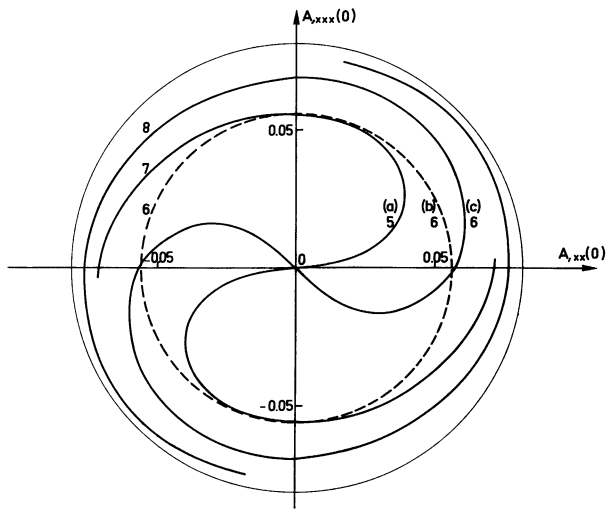

Fig. 3*a*. — The trace in P_2 of the starting points for solution in a finite box (for $\varepsilon = 0.1$), (*a*) corresponds to odd solutions (with respect to the middle of the box), (*b*) to solution without parity and (*c*) to even solutions. The outside circle is the set of starting points for half-infinite solutions.

Accordingly, when one plots (at fixed ε) the bulk wavelength as a function of L, one gets in the (L, λ) Cartesian plane a curve oscillating between the two extreme values of λ, say λ_+ and λ_-, which are the boundaries of the accessible band of SCT. As shown on figure 3*b*, these oscillations are of period λ_+ (resp. λ_-) when the wavelength takes its maximum (resp. minimum) value. By continuity, a branch of solution in the (L, λ) plane keeps its number of nodes constant as far as its wavelength does not reach λ_+ as L grows. The lower limit of the branch corresponds to $A_{xxx} = 0$ in P_2 ; this corresponds too to the maximum for the invariant and to the minimum for λ. As shown in figure 3*b*, the curve giving λ as a function of L is obtained by joining all these branches and accounting for the bifurcations between symmetric, antisymmetric and nonsymmetric solutions.

As L increases at fixed ε, the number of oscillations in λ_+ grows as L/λ_+ although the number of oscillations of period λ_- is L/λ_-. Hence, the number of intercepts of the multivalued curve $\lambda(L)$ with a vertical line $L = C$ is of order unity as $\varepsilon^{-1/2} \lesssim L \lesssim \varepsilon^{-1}$, and becomes of order $L\left(\frac{1}{\lambda_-} - \frac{1}{\lambda_+}\right) \sim L\varepsilon$ for $L \gg \varepsilon^{-1}$.

Furthermore, solutions without symmetry with respect to the middle of the box exist. They do not appear by linear bifurcation from the $A = 0$ state, unless ε and L take special values for which the ground state of the linear problem is degenerated. These unsymmetrical solutions as viewed in P_2 connect the successive crossing of the two above defined spirals with the axis $A_{xx} = 0$ and $A_{x^3} = 0$ (see Fig. 3*a*). They are defined by initial conditions on a set of more or less concentric closed lines tending asymptotically to Γ as L increases.

In model (*a*), once a solution exists for (ε, L) given, it keeps the same wavenumber as ε grows. This is understood by looking at the (multivalued) plot of λ as a function of L.

In this plot, each solution is at the crossing of a line $L = C$ with a branch of solutions ; that is, a line joining two extremal values of the wavelength $\lambda_\pm(\varepsilon)$. As ε increases, λ_+ increases and λ_- decreases. Thus, the upper limit of all branches of solutions move toward increasing L, and the lower limit toward decreasing L. The ratio of the displacements of these two limits is constant near $\varepsilon = 0_+$, as both λ_- and λ_+ differ from $2\pi/q_0$ by a quantity of order ε. Thus the intercept of any branch with a line $L = C$ remains approximately at the same wavelength as ε increases. One may also notice that no new node appears (or disappear) in a solution as far as it has not reached one of the extremal values $\lambda_\pm$.

In model (*b*) both λ_+ and λ_- increase as ε increases, and the upper and lower limits of any branch of solution move towards decreasing L in the (L, λ) plane [15]. There is a succession of bifurcations

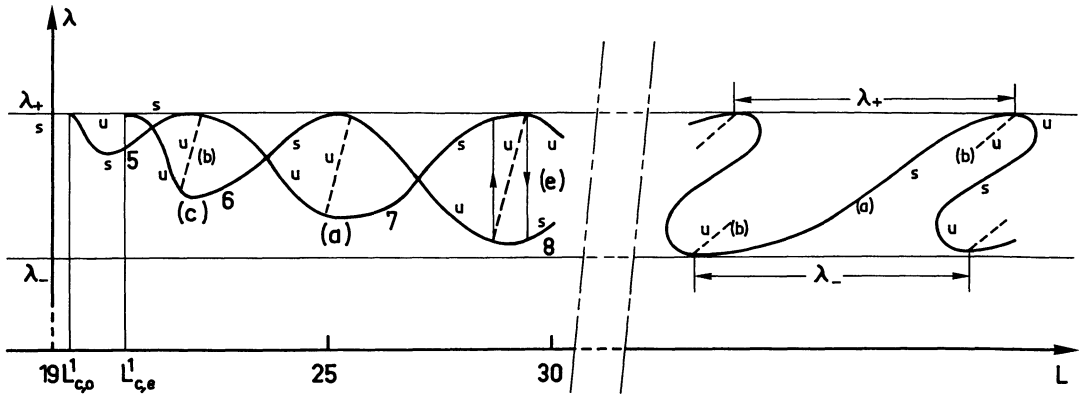

Fig. 3*b*. — This is the bulk wavelength of finite solutions as a function of their total length (again for $\varepsilon = 0.1$). The wavelength oscillates (for L large enough with respect to $\varepsilon^{-1/2}$) between λ_- and λ_+. They are two oscillating curves corresponding to even and odd solutions (with respect to the middle of the cell). For large L only even solutions are shown. s is for stable and u for unstable and a possible hysteresis loop is drawn (e). For large L as the period of the upper oscillations (on λ_+) is λ_+ and of the lower ones is λ_-, the whole representation curve $\lambda(L)$ is twisted and the number of solutions for L fixed becomes of order $L\left(\frac{1}{\lambda_-} - \frac{1}{\lambda_+}\right)$.

(L fixed, ε increasing) each one occurring whenever the upper or lower limit of a branch of solution crosses the vertical line $L = C$. Thus the wavenumber jumps (and decreases) by small increments, staying close (at a distance $\sim L^{-1}$) to the curve $2\pi\lambda_-^{-1}(\varepsilon)$ in the (q, ε) plane as ε increases. Actually a subcritical bifurcation takes place whenever the line $2\pi\lambda_-^{-1}(\varepsilon)$ is reached in the (q, ε) plane, and it is natural to assume that the solution jumps toward the stable solution with the nearest wavenumber (and so changes its parity with respect to the middle of the cell). Each jump corresponds to the destruction of a « roll » near the boundary. This description is in fair agreement with the often noticed (but yet unexplained) fact that adjustment of the wavenumber occurs through the nucleation or destroying of rolls at the lateral boundaries.

Similarly, as ε decreases in model (*b*) (but εL remaining large) the wavenumber remains close to the line $2\pi\lambda_+^{-1}(\varepsilon)$. Of course various hysteretic phenomena can in principle exist if ε is varied in a more or less complicated way.

4. **Final remarks.** — As conclusion we discuss a few points raised by our results.

4.1. — First of all, owing to our use of a « geometrical » method, one may wonder how much our results depend on peculiarities of our models. Actually, the « realistic » problems of wavelength selection in cellular flows implies at least the existence of another space-dimension (for instance the vertical dimension in gravity controlled Rayleigh-Bénard convection) so that the steady state equations are by themselves (i.e. without time dependence) partial differential equations (instead of ordinary differential equations as in our models). We believe that this does not affect our main qualitative results (i.e. that the lateral boundary conditions control the wavelength and restrict it to a band of width $\sim \varepsilon$). Looking carefully at our method, one notices that it uses essentially the matching of the inner and outer envelope solution. And, precisely, this approach remains valid even if there is a structure along the vertical direction : this vertical structure accomodates slow changes in the horizontal amplitude with a characteristic length of the order of the wavelength. Thus one may forget in some sense this supplementary dimension and limit oneself to variations in the horizontal dimension.

However, it remains to carry out our analysis in a « realistic » situation [19] (for instance the Rayleigh-Bénard convection between rigid boundaries).

4.2. — The idea of a realistic treatment of the pattern selection in Rayleigh-Bénard convection could be more elusive than it appears first. Actually it is not at all certain that experiments without any forcing process (as a horizontal temperature gradient forcing a roll at lateral boundaries or an imposed thermal grid) yield, near threshold, well defined rolls parallel to the boundaries, when the aspect ratio in rectangular geometry becomes large both *along* and *perpendicular* to the rolls. This is precisely the configuration which could be treated more easily by the theory : i.e. the case of long (in principle infinitely long) rolls limited by rigid vertical boundaries. In real experiments with large aspect ratio and without forcing of the structure, most of the time complicated patterns [16] are obtained ; these cannot nevertheless be considered to be random, since they exhibit well definite symmetries with respect to the box geometry. To be truly « realistic » one should solve the (formidable) problem of selection of these complicated patterns. For the moment, the only reasonable guess we can make about these structures is that near threshold the rolls are always perpendicular (or eventually parallel) to the boundaries. This is likely a manifestation of the well known property that the nodal lines of the solution of the Helmholtz equa-

tion $[(\Delta + k_0^2)\,\psi = 0]$ in a 2-d box with Dirichlet boundary conditions ($\psi = 0$) cut perpendicularly the boundaries when their curvature is much smaller than k_0.

4.3. — The case of model (*a*) seems easier to treat, at least at first glance, since one can assume that the selected pattern is the one with the lowest potential. From this point of view too this is certainly not a good model for standard problems in cellular flows, wherein the evolution equations (say the Oberbeck-Boussinesq equations) have no variational structure.

One of the conclusion which can be drawn from our calculations is that, among all steady solutions without internal envelope node, one is the most stable, having the minimum potential. Of course this is the one with wavenumber closest to the optimal wavelength [7] (at a distance of order L^{-1}, as the possible wavenumbers are quantized in the band

$$]q_0 + \delta_-(\varepsilon),\, q_0 + \delta_+(\varepsilon)[\,,$$

the quantum being L^{-1}). However this does not tell us that solutions with a wavenumber differing from the optimal one are linearly stable or unstable. It is possible that they lie at a local minimum of the potential. Perhaps the height of the potential barrier separating two such solutions is of order of the contribution of one wavelength of solution to the potential.

Furthermore, the case of solutions in rectangular boxes is much more complicated, as the minimum of potential could be reached for a quite irregular pattern. Solutions of the linear part of our equations in rectangular boxes have been found [17] with dislocations. These solutions in the non linear regime could have a lower potential than the regular ones, owing for instance to a lower contribution from the lateral boundary layers. The fact that the rolls in Rayleigh-Bénard convection tend to be perpendicular to the larger side of the cell indicates that under quite general conditions the « energy » of this configuration is lower than the one of rolls parallel to the vertical boundaries. Accordingly it could be better, from this energetic point of view, to have rolls everywhere perpendicular to lateral boundaries, at the price of a few internal dislocations. In two dimensional elasticity theory, the energy of dislocations grows as the logarithm of the sample size and this should be negligible with respect to the boundary energy, implying quantities of the order of the sample size itself.

4.4. — Concerning the search of realistic boundary conditions, another remark is of some interest. In our model (*a*) (and this is presumably a quite general feature), the boundary layer (when the rolls are parallel to the lateral boundary) is unstable against a localized (in the x direction, the roll and the lateral boundary being parallel to the y direction) cross-roll instability.

Let $A_0(x)$ be a half-infinite solution for model (*a*) limited at $x = 0$ by a rigid boundary ($A = A_x = 0$ at $x = 0$), and consider a linear perturbation in the form $e^{\hat{\sigma}t}\,\alpha(x)\sin q_0 y$. This is made of rolls perpendicular to the main rolls. If $\alpha(x)$ varies slowly with x one may neglect its rapid variation, as implying higher harmonics of a negligible amplitude near $\varepsilon = 0$, and obtain from (1*a*) for this slowly varying part the linearized equation

$$\varepsilon\alpha - \alpha_{xxxx} - 2\,\varepsilon \tanh^2\left(\frac{x\varepsilon^{1/2}}{\xi_0}\right)\alpha = \hat{\sigma}\alpha \qquad (15)$$

where we have written the unperturbed solution as

$$A_0(x) = \pm\left(\frac{4\,\varepsilon}{3}\right)^{1/2} \sin q_0 x \tanh\left(\frac{x\varepsilon^{1/2}}{\xi_0}\right).$$

This equation is to be supplemented by the usual b.c. $\alpha = \alpha_x = 0$ at $x = 0$. Let us dimensionalize this equation by $x = X\varepsilon^{-1/4}$ and put $\hat{\sigma} = \sigma\varepsilon$, so that (15) becomes

$$\alpha - \alpha_{XXXX} - 2\tanh^2\left(\frac{X\varepsilon^{1/4}}{\xi_0}\right)\alpha = \sigma\alpha\,. \qquad (16)$$

The largest eigenvalue σ is given by the Rayleigh-Ritz formula

$$\sigma = \max_{\alpha(X)} \frac{\left(\alpha,\, \left(1 - 2\tanh^2\left(\frac{X\varepsilon^{1/4}}{\xi_0}\right)\right)\alpha\right) - (\alpha_{XX}, \alpha_{XX})}{(\alpha, \alpha)} \qquad (17)$$

where $(f, g) \equiv \int_0^\infty f(x)\,g(x)\,dx$, and the maximum is taken on test function satisfying the b.c. ($\alpha = \alpha_x = 0$ at $x = 0$). It is easy to show that σ tends to 1 as ε tends to zero.

If one neglects the $\tanh^2$ term in (16), $\sigma = 1$ is an eigenvalue with the eigenfunction x^3. Inserting a test function of the form $x^3\,e^{-\eta x}$ into the right hand side of (17) one establishes the instability.

It should be also noticed that this sort of perpendicular modulation of the boundary rolls is quite often observed in experiments [16].

4.5. — Last but not least, our model allows one to check carefully many details of our analysis. In particular, it confirms in a detailed fashion the validity of the amplitude approach for the questions under consideration. Moreover our results are in agreement with those already obtained [5] reaching the final steady state in a box by numerical integration of the dynamics.

Acknowledgments. — The authors are indebted to Pierre Hohenberg for many discussions which greatly helped them to clarify a number of points.

Appendix A. — In this appendix, we explain how to compute the tangent structure to the SCT in model (*a*). This shows in particular that near $\varepsilon = 0_+$ the trajectories with a wavenumber in the Eckhaus unstable range are elliptic, although the Eckhaus stable ones are hyperbolic.

First of all, let us notice that for a given value of the invariant K, they are either one, two or zero SCT. The marginal case (one SCT) corresponds to the boundary of the Eckhaus stability region. Near $\varepsilon = 0_+$ the value of the invariant as a function of $\delta = q - q_0$ (q being the wavenumber of the solution) is

$$K = \tfrac{1}{6}(\varepsilon - 4\, q_0^2\, \delta^2)\,[\varepsilon + 16\, q_0^3\, \delta + \mathcal{O}(\delta^2)]\,. \quad (A.1)$$

The marginal case (one value of δ for one value of K) corresponds to $dK/d\delta = 0$, which gives

$$\varepsilon \simeq 12\, q_0^2\, \delta^2 + \mathcal{O}(\delta^3)\,.$$

This is precisely the boundary of the region of Eckhaus stability.

To find the tangent structure of the SCT, one proceeds as follows. Let

$$A(x) = a_0 \sin qx + a_1 \sin 3\, qx \quad (A.2)$$

be the steady function of (1*a*) with wavenumber q. One considers a small perturbation around this solution of the general form

$$\overline{A}(x) = e^{\sigma x}(\overline{a}_0 \sin qx + \overline{a}_1 \sin 3\, qx + \overline{b}_0 \cos qx + \overline{b}_1 \cos 3\, qx)\,. \quad (A.3)$$

To proceed with the following calculation, it is useful to notice a few formal relations.

Let us put $v(x) = (\alpha \cos qx + \beta \sin qx)\, e^{\sigma x}$ and

$$v^1(x) = (-\alpha \sin qx + \beta \cos qx)\, e^{\sigma x}\,,$$

α and β arbitrary numbers. Thus

$$\Omega_\varepsilon\, v = [\varepsilon - (\sigma^2 - q^2 + q_0^2)^2 + 4\, \sigma^2\, q^2]\, v + 4\, \sigma q(\sigma^2 - q^2 + q_0^2)\, v^1\,.$$

One is looking for a solution of

$$\Omega_\varepsilon\, \overline{A} - 3\, A^2\, \overline{A} = 0 \quad (A.4)$$

where A and $\overline{A}$ are given in (A.2) and (A.3).

By identification of the coefficients of the various circular functions of qx in (A.4) one gets homogeneous systems in $\overline{a}_0$, $\overline{a}_1$, $\overline{b}_0$ and $\overline{b}_1$. At the lowest order in ε, this yields

$$[\varepsilon - (\sigma^2 - q^2 + q_0^2)^2 + 4\, \sigma^2\, q^2 - \tfrac{9}{4} a_0^2 + \tfrac{3}{2} a_0 a_1]\, \overline{a}_0 - 4\, \sigma q(\sigma^2 - q^2 + q_0^2)\, \overline{b}_0 + \tfrac{3}{4} a_0^2\, \overline{a}_1 = 0\,,$$

$$[\varepsilon - (\sigma^2 - 9\, q^2 + q_0^2)^2 + 36\, \sigma^2\, q^2 - \tfrac{3}{2} a_0^2]\, \overline{a}_1 - 126\, q(\sigma^2 - 9\, q^2 + q_0^2)\, \overline{b}_1 + (\tfrac{3}{4} a_0^2 - 3\, a_0 a_1)\, \overline{a}_0 = 0$$

and two similar relations. The whole (homogeneous) system has a non trivial solution if its determinant is non zero, this giving an equation for σ.

This equation has the form (by neglecting terms of higher order in ε)

$$\left[\sigma^4 - 2(3\, q^2 - q_0^2)\, \sigma^2 + 2\, \gamma(q) + \frac{3}{2}\frac{\gamma(q)^2}{\gamma(2\, q)}\right]\left[\sigma^4 - 2(3\, q^2 - q_0^2)\, \sigma^2 + \frac{1}{2}\frac{\gamma(q)^2}{\gamma(2\, q)}\right] + \sigma^2\left[4\, q(\sigma^2 - q^2 + q_0^2) + \frac{24\, q_0^2\, \delta\gamma(q)^2}{\gamma(2\, q)^2}\right] \quad (A.5)$$

where $\gamma(z) = \varepsilon - (z^2 - q_0^2)^2$.

After expanding this equation, one finds that to the lowest order in ε, a pair of Floquet exponents becomes equal to zero if $\varepsilon = 12\, q_0^2\, \delta^2$. This corresponds to the value of δ for which these Floquet exponents change from real to imaginary values, and precisely to the curve of marginal Eckhaus stability in (q, ε). Furthermore the fact that (A.5) is even with respect to σ comes basically from the space reversal symmetry of the original equation that exchanges the stable and unstable manifolds, and this shows that these manifolds are two-dimensional.

The calculations in model (*b*) can be done along very similar lines and show similarly that the elliptic-hyperbolic boundary for the tangent structure of the SCT is at the marginal Eckhaus stability.

Appendix B. — In this appendix, we compute the adiabatic invariant for the system (*b*) near $\varepsilon = 0_+$ [this invariant plays the same role as the exact invariant K for the model (*a*) for the determination of the accessible SCT]. Let $J(A)$ be this invariant. It could be obtained in principle by multiplying the equation

$$\varepsilon A - (\partial_{x^2}^2 + q_0^2)^2\, AA_x = 0 \quad (B.1)$$

by A_x, integrating over one period $2\,\pi/q$, q being some « local » wavenumber of the solution which

should not be strictly periodic either. In this way one should get a small variation of $J(A)$, connected with the weak non periodicity of the solution. This small variation were the x-derivative of the sought adiabatic invariant.

This procedure is uneasy to follow in practice, because a number of contributions might be easily missed. We have preferred to proceed as follows : first the linear part of the left hand side of (B.1) generates the following quadratic contribution to this invariant, which is straightforward :

$$J^1(A) = \varepsilon \frac{A^2}{2} - q_0^4 \frac{A^2}{2} - q_0^2 A_x^2 - A_x A_{xxx} + \frac{1}{2} A_{xx}^2$$

the value of this part of the invariant, as a function of the wavenumber q for the SCT is near $\varepsilon = 0_+$ and $q = q_0$:

$$J^1(A) = \frac{1}{4}(a_0')^2 \left(\frac{16\,\varepsilon}{3} + 8\, q_0^3\, \delta \right)$$

where a_0' is the amplitude that appears in the expansion (2*b*) and where $\delta \equiv q - q_0$. Near $\varepsilon \simeq 0_+$ and for $\delta \sim 0(\varepsilon)$ the approximate form of $J^1(A)$ is

$$J^1(A) = 72\, \varepsilon q_0^2 \left(\frac{2\,\varepsilon}{3} + q_0^3\, \delta \right).$$

It remains to consider the contribution of AA_x to $J(A)$. We assume that the solution $A(x)$ is the product of a rapidly varying function of x times a slowly varying amplitude. This expansion is to be combined with the usual power expansion in ε : the *a priori* form of $A(x)$ is taken as

$$A = A^{(1)}(x) + A^{(2)}(x) + \cdots$$

where the superscript (1), (2), ... refers to the (formal) order in ε. Moreover $A^{(1)}(x)$ expands as

$$A^{(1)}(x) = \chi(x) \sin q_0\, x + \tilde{\chi}(x) \cos q_0\, x + \cdots \quad \text{(B.2)}$$

where now the expansion is with respect to the small derivative of χ, so that $\tilde{\chi} \sim \chi_x$.

The second harmonic $A^{(2)}$ is the solution of

$$\varepsilon A^{(2)} - (\partial_{x^2}^2 + q_0^2)^2 A^{(2)} = [A^{(1)} A_x^{(1)}]_2 \quad \text{(B.3)}$$

where $[A^{(1)} A_x^{(1)}]_{(2)}$ is made of circular function either of argument $2\, q_0\, x$ or 0 (for what concerns the « rapid » variation). The solution of (B.3) must be obtained up to first order in χ_x (which is also the order of $\tilde{\chi}$).

The corresponding result is inserted into the equation for $A^{(1)}$:

$$\varepsilon A^{(1)} - (\partial_{x^2}^2 + q_0^2)^2 A^{(1)} = [A^{(1)} A_x^{(2)} + A^{(2)} A_x^{(1)}]_1 \quad \text{(B.4)}$$

where the subscript (1) means that we keep the contributions from $\sin q_0\, x$ and $\cos q_0\, x$ only (and neglect $\sin 3\, q_0\, x$, ...). By identification of the coefficients of these circular functions in (B.4), one gets both the self consistent amplitude equation for χ and the value of $\tilde{\chi}$ as a function of χ_x and χ.

The final step consists in writing $A^2 A_x$ (which is to be integrated over one period to get the non linear part of the adiabatic invariant) up to terms of first order in χ_x. This quantity can thus be written as the (slow) derivative with respect to x of some function of χ, yielding the desired contributions to the adiabatic invariant.

We give below some details about this calculation. It is understood tacitly at each step that terms of relevant order only are considered.

The first step in the calculation (i.e. the solution of (B.3)) gives, near $\varepsilon = 0_+$

$$A^{(2)} = \frac{1}{\gamma(2\, q_0)} \times \times \left[\frac{1}{2} q_0\, \chi^2 \sin 2\varphi + \frac{13}{6} \chi \chi_x \cos 2\varphi + q_0\, \chi \tilde{\chi} \cos 2\varphi \right] + \frac{\chi \chi_x}{\gamma(0)} \quad \text{(B.5)}$$

where $\gamma(z) \equiv \varepsilon - (z^2 - q_0^2)^2$ and $\varphi \equiv q_0\, x$. This calculation is not completely straightforward, as one must take care (for instance) that the solution of $f_x = \chi^2 \sin 2\, q_0\, x$ is (when χ depends slowly on x)

$$f = -\frac{\chi^2 \cos 2\, q_0\, x}{2\, q_0} + \frac{\chi \chi_x}{2\, q_0^2} \sin 2\, q_0\, x + \cdots$$

By comparison of (B.2) and (B.5), one notices that the (small) term $\tilde{\chi} \cos \varphi$ in (B.2) is merely a local phase change in the rapid variation. Actually, if $\tilde{\chi}$ is small with respect to χ (as it should be), $A^{(1)}$ can be written $A^{(1)} \simeq \chi \sin \left(q_0\, x + \frac{\tilde{\chi}}{\chi} \right)$. The same phase change, once done into the dominant term of $A^{(2)}$ $\left[\text{i.e. } \frac{q\chi^2}{2\,\gamma(2\, q_0)} \sin 2\, q_0\, x \right]$ yields $\frac{\chi \tilde{\chi}}{\gamma(2\, q_0)} \cos (2\, q_0\, x)$ which is exactly the contribution proportional to $\tilde{\chi}$ on the right hand side of (B.5). This explains why no contribution from $\tilde{\chi}$ may appear in the adiabatic invariant, as this invariant must be insensitive to a global change of phase of the fast oscillations. Such a contribution appears at the order of the gradient of this phase only, and thus is of higher order.

To go further, we completely neglect terms arising from this phase shift, as they ultimately compensate in the adiabatic invariant. The quantity to be computed is thus the slowly varying part of

$$M(A) \equiv A(A_x)^2 . \quad \text{(B.6)}$$

By substituting the expansion $A = A^{(1)} + A^{(2)} + \cdots$ into (B.6), one gets (at the dominant order of course)

$$M(A) = A^{(2)}(A_x^{(1)})^2 + A_x^{(2)}(A^{(1)})_x^2 .$$

Neglecting, as explained above, all the contributions arising from $\tilde{\chi}$ (although they are formally of the same order as the ones under consideration), one has

$$(A^{(1)})_x^2 = q_0\,\chi^2 \sin 2\varphi + \chi\chi_x(1 - \cos 2\varphi)$$

and

$$A_x^{(2)} = \frac{1}{\gamma(2\,q_0)}\left(q_0^2\,\chi^2 \cos 2\varphi - \frac{10}{3}\,q_0\,\chi\chi_x \sin 2\varphi\right)$$

thus

$$\overline{(A^{(1)})_x^2\,A_x^{(2)}} = -\frac{13\,q_0^2}{6\,\gamma(2\,q_0)}\quad \chi^3\,\chi_x = \frac{13}{54\,q_0^2}\,\chi^3\,\chi_x \qquad (B.7.a)$$

where the horizontal bar denotes the average over the fast variation ($\overline{\cos^2\varphi} = \frac{1}{2}$, ...).

Similarly

$$(A_x^{(1)})^2 = \frac{q_0^2\,\chi^2}{2}(1 + \cos 2\varphi) + \chi\chi_x \sin 2\varphi\,.$$

This yields, after multiplication with (B.5) (and by omitting again terms proportional to $\tilde{\chi}$)

$$A^{(2)}(A_x^{(1)})^2 = q_0^2\,\chi^3\,\chi_x\left(\frac{19}{24\,\gamma(2\,q_0)} + \frac{1}{4\,\gamma(0)}\right)$$

$$= -\frac{73\,\chi^3\,\chi_x}{216\,q_0^2}$$

so that

$$\overline{M(A)} = -\frac{\partial}{\partial x}\left(\frac{7\,\chi^4}{288\,q_0^2}\right) \qquad (B.7.b)$$

which implies that the corresponding contribution to the adiabatic invariant is $7\,\chi^4/288\,q_0^2$. Its value for the SCT with a wavenumber close to q_0 is (remind $\chi^2 \simeq 36\,\varepsilon q_0^2)\,\frac{63}{2}\,\varepsilon^2\,q_0^2$.

Keeping together this non linear contribution with the one of the quadratic term, one has (again for the SCT of wavenumber $q_0 + \delta$) :

$$J(A) = 48\,\varepsilon q_0^2\left(\varepsilon + \frac{48}{53}\,q_0^3\,\delta\right). \qquad (B.8)$$

References

[1] Lord RAYLEIGH, *Philos. Mag.* **56**, **32** (1916) 529.

[2] It is now well known that the cells of Bénard were due to capillary phenomena, and not to the buoyancy driven convection studied by L. Rayleigh. See for instance BLOCK, M. J., *Nature* (London) **178** (1956) 650 ; PEARSON, J. R., *J. Fluid. Mech.* **4** (1958) 489 ; SCRIVEN, L. E. and STERLING, C. V., *J. Fluid Mech.* **19** (1964) 321.

[3] KOSCHMIEDER, E. L., *Adv. Chem. Phys.* **26** (1974) 177 and references quoted therein.

[4] AHLERS, G. and BEHRINGER, R. P., *Phys. Rev. Lett.* **40** (1978) 712.
LIBCHABER, A. and MAURER, J., *J. Physique Lett.* **39** (1978) L-369.

[5] MANNEVILLE, P. and POMEAU, Y., *Phys. Lett.* **A 75** (1979) 296.

[6] SOROKIN, V. C., *Priklad. Mat. i Mek.* **17** (1953) 39.

[7] POMEAU, Y. and MANNEVILLE, P., *J. Physique Lett.* **40** (1979) L-609.

[8] CROSS, M. C., DANIELS, P. G., HOHENBERG, P. C. and SIGGIA, E. D. (unpublished), private communication from HOHENBERG, P. C.

[9] MANNEVILLE, P., Private communication.

[10] ECKHAUS, W., *Studies in non linear stability theory* (Springer-Verlag, New York) 1965.

[11] See for instance appendix 8 in ARNOLD, V., *Méthodes mathématiques de la mécanique classique* (Ed. Mir, Moscou) 1976.

[12] AUBRY, S., in *Bifurcation phenomena in mathematical physics and related topics*, C. Bardos, D. Bessis eds. (D. Reidel Pub. Dordrecht).

[13] IOOSS, G., *Bifurcation of maps and applications* (North Holland Math. Studies **36** New York) 1979.

[14] SEGEL, L. A., in *Non equilibrium thermodynamics : Variational techniques and stability*, R. J. Donnelly, I. Prigogine and R. Hermann eds. (Univ. of Chicago Press) 1966.

[15] We have been informed by P. Hohenberg that the method which was presented in reference [8] has led these authors to the same result.

[16] BERGÉ, P., CROQUETTE, V., DUBOIS, M., Private communication.

[17] NORMAND, C., *Convection flow patterns in rectangular boxes of finite extend* Preprint CEA/DPh. T 49, May 1980 and to appear in Z.A.M.P.

[18] CHEN, M. M., WHITEHEAD, J. A., *J. Fluid Mech.* **31** (1963) 1.

[19] The wavelength selection in R.B. convection by the boundary effects has been treated near threshold in reference [8] for the case of free-free horizontal b.c. and rigid vertical boundaries. The buckling of long rectangular plates poses a similar problem and has been solved near threshold by the method exposed in the present paper [POMEAU, Y., *Non linear pattern selection in a problem of elasticity* preprint CEA/DPh.T/103/80, published in *J. Physique Lett.* **42** (1981) L-1].

[20] POMEAU, Y., ZALESKI, S., Communication at the *Colloque Pierre Curie* Paris (Sept. 1980), to be published.

[21] DANIELS, P. G., *Proc. R. Soc. London* **A 358** (1977) 173 and HALL, P., WALTON, I. C., *Proc. R. Soc. London* **A 358** (1977) 199.